crystals

MDPI

Article

5-Fluorocytosine/Isocytosine Monohydrate. The First Example of Isomorphic and Isostructural Co-Crystal of Pyrimidine Nucleobases

Gustavo Portalone

Department of Chemistry, 'Sapienza' University of Rome, 00185 Rome, Italy; gustavo.portalone@uniroma1.it; Tel.: +396-4991-3715

Received: 1 October 2020; Accepted: 2 November 2020; Published: 3 November 2020

Abstract: To date, despite the crucial role played by cytosine, uracil, and thymine in the DNA/RNA replication process, no examples showing isomorphic and isostructural behavior among binary co-crystals of natural or modified pyrimidine nucleobases have been so far reported in the literature. In view of the relevance of biochemical and pharmaceutical compounds such as pyrimidine nucleobases and their 5-fluoroderivatives, co-crystals of the molecular complex formed by 5-fluorocytosine and isocytosine monohydrate, $C_4H_4FN_3O{\cdot}C_4H_5N_3O{\cdot}H_2O$, have been synthesized by a reaction between 5-fluorocytosine and isocytosine. They represent the first example of isomorphic and isostructural binary co-crystals of pyrimidine nucleobases, as X-ray diffraction analysis shows structural similarities in the solid-state organization of molecules with that of the (1:1) 5-fluorocytosine/5-fluoroisocytosine monohydrate molecular complex, which differs solely in the H/F substitution at the C5 position of isocytosine. Molecules of 5-fluorocytosine and isocytosine are present in the crystal as 1*H* and 3*H*-ketoamino tautomers, respectively. They form almost coplanar WC base pairs through nucleobase-to-nucleobase DAA/ADD hydrogen bonding interactions, demonstrating that complementary binding enables the crystallization of specific tautomers. Additional peripheral hydrogen bonds involving all available H atom donor and acceptor sites of the water molecule give a three-dimensional polymeric structure. In the absence of H···F hydrogen-bonding interactions, the robustness of the supramolecular architectures based on three-point recognition synthons is responsible for the existence of isostructurality between the two molecular complexes.

Keywords: nucleobases; 5-halonucleobases; cytosine; 5-fluorocytosine; base pairs; hydrogen bond; binary co-crystals; isomorphism; isostructurality

1. Introduction

In the formation of binary co-crystals, a second substance may be incorporated into the crystal lattice by replacing the molecules of the first component, leaving unit-cell dimensions and space groups unaltered (isomorphism). This can happen particularly if molecules of the two substances are structural homologues. However, isomorphism does not necessarily imply isostructurality, i.e., the situation where two crystal structures of different chemical composition exhibit the same spatial arrangement of molecules, in the formation of crystals or co-crystals [1,2]. Although small changes in the molecular structure can significantly affect molecular disposition in the crystal, specific functional groups or atoms can be interchanged without modifying crystal packing, provided that such groups (or atoms) are not involved in hydrogen bonds [3]. Concerning the exchange of the hydrogen/fluorine atoms, a systematic investigation in the Cambridge Structural Database (CSD) of almost 125,000 pairs of crystal structures yielded 645 pairs containing molecules which differed only in the substitution of H with F atoms, and 21% of them showed structural similarities in the solid-state organization [4].

Considering this, and the fact that the properties of molecular substances in the solid state depend essentially on their chemical nature, their stoichiometry and their reciprocal disposition in space, from the structural chemistry point of view pyrimidine nucleobases and their fluorosubstituted derivatives deserve special attention. On one side, the fundamental importance of cytosine, uracil, and thymine for structural molecular biology and supramolecular chemistry has been well-known for decades. On the other hand, it has been shown that the formation of haloderivatives of cytosine in DNA can be responsible for several modifications in the structure of DNA observed in human tumors [5], and mass spectrometry has been applied to detect halocytosines as free nucleobases to evaluate cytosine halogenation as an endogenous mutagenic pathway in human tissue [6]. Therefore, it is surprising that hardly any example showing isomorphic and isostructural behaviors between co-crystals of natural pyrimidine nucleobases and co-crystals of their fluorosubstituted derivatives can be found in the literature. In addition, although isostructurality is relatively common in crystals of multi-component systems, the author's literature search found only four cases of crystal packing similarity of centro/noncentrosymmetric co-crystals formed by pyrimidine nucleobases/5-fluorosubstituted derivatives with polymorphic centro/noncentro symmetric crystals of the 5-fluorosubstituted coformers. These four examples (Scheme 1), in which there was no indication of C–H···F intermolecular interactions, refer to the crystal structures of:

i) the monoclinic $P2_1/c$ forms of monohydrate (1:1) 5-fluorocytosine/cytosine, SAVKIM [7], and monohydrate 5-fluorocytosine, BIRMEU02 [8];
ii) the monoclinic $P2_1/n$ forms of (1:1) 5-fluorocytosine/cytosine, ADAJAT [9], and 5-fluorocytosine, MEBQEQ [8];
iii) the tetragonal $P4_12_12$ forms of (1:1) 5-fluorocytosine/cytosine, ADAJAT01 [9], and 5-fluorocytosine, MEBQEQ01 [8];
iv) the orthorhombic *Pnma* forms of (1:1) *N*,*N*-dimethyluracil/*N*,*N*-dimethyl-5-fluorouracil, *N*,*N*-dimethyl-5-fluorouracil, OKATEB and KAMSAS01, respectively [10], and *N*,*N*-dimethyluracil, DMURAC01 [11].

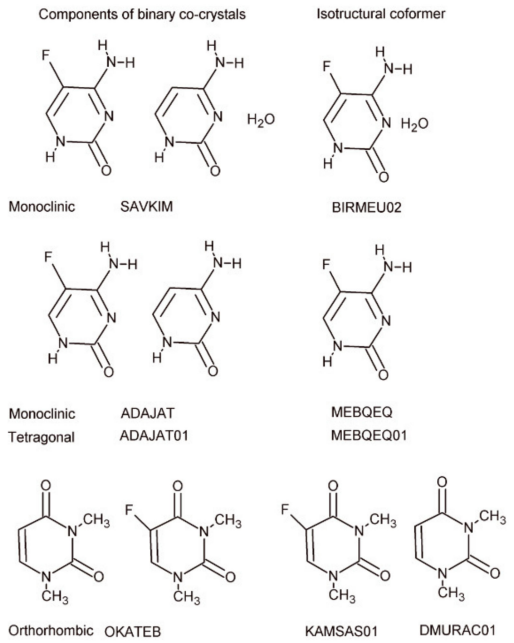

Scheme 1. Components of the binary co-crystals of pyrimidine nucleobases/5-fluorosubstituted derivatives showing crystal packing similarity with unsubstituted and 5-fluorosubstituted conformers.

Notably, in all the crystal structures of the isostructural pairs SAVKIM/BIRMEU02, ADAJAT/MEBQEQ and ADAJAT01/MEBQEQ01 5-fluorocytosine and cytosine are present as

1*H*-ketoamino tautomers. Consequently, the DAA/ADD triple hydrogen bond interaction between nucleobases is precluded, and dimerization is obtained through two independent DA/AD interactions based on the same constituent hydrogen bonds: (ring)N–H···N(imino) and (amino)N–H···O (carbonyl) (Figure 1).

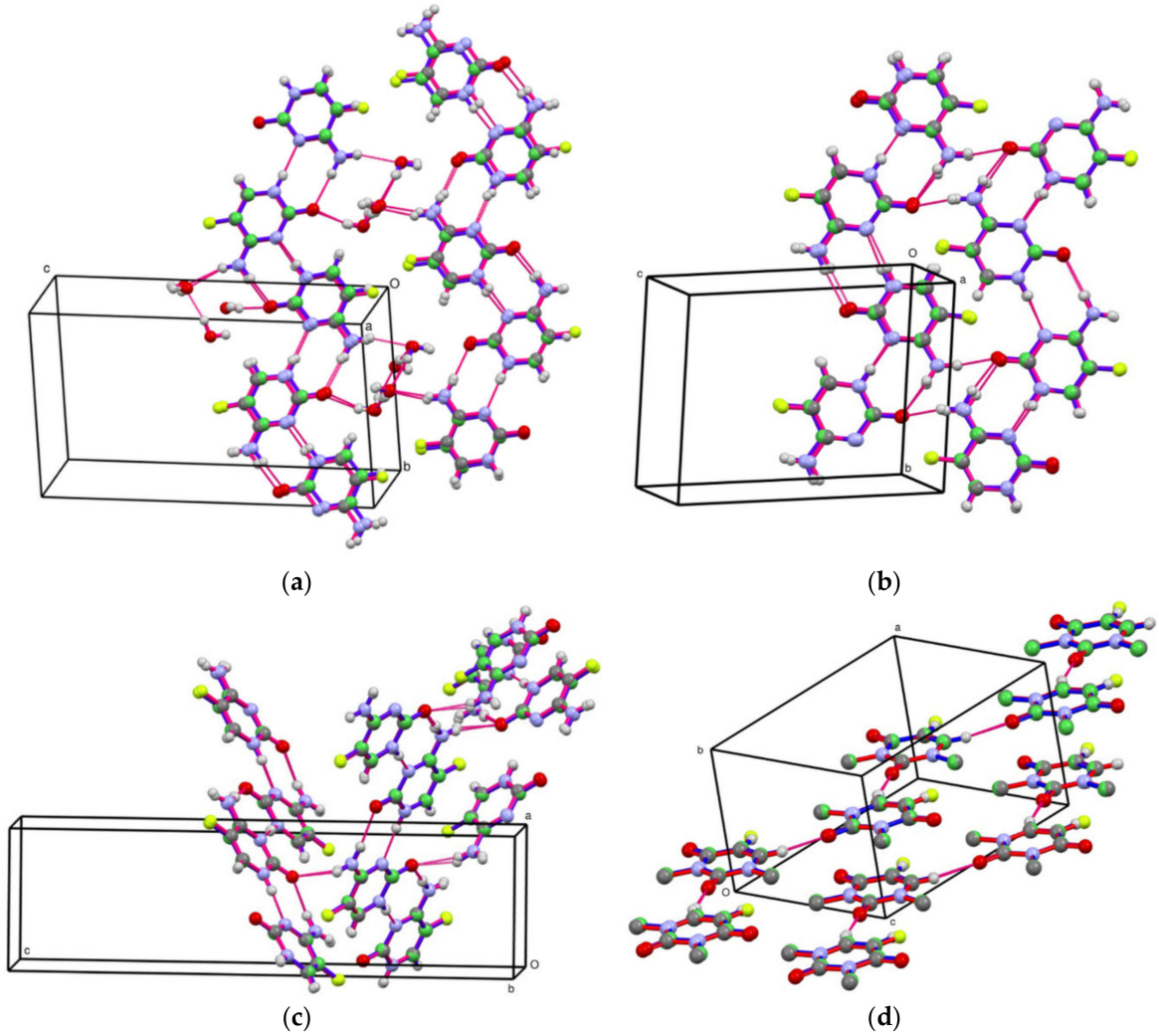

Figure 1. Overlay of part of the crystal structure showing crystal packing similarity for: (**a**) BIRMEU02 and SAVKIM, viewed approximately down *a*. Bonds of molecules of BIRMEU02 have been colored red, and bonds of molecules of SAVKIM are blue. (**b**) MEBQEQ and ADAJAT, viewed approximately down *a*. Bonds of molecules of MEBQEQ have been colored red, and bonds of molecules of ADAJAT are blue. (**c**) MEBQEQ01 and ADAJAT01, viewed approximately down *b*. Bonds of molecules of MEBQEQ01 have been colored red, and bonds of molecules of ADAJAT01 are blue. (**d**) KAMSAS01 and OKATEB, viewed approximately down *b*. Bonds of molecules of KAMSAS01 have been colored red, and bonds of molecules of OKATEB are blue. For the sake of simplicity, overlay of part of the crystal structure of the pairs DMURAC01/OKATEB and KAMSAS01/DMRAC01, similar to that of the pair KAMSAS01/OKATEB, has been omitted. All atoms are shown as small spheres of arbitrary radii. Hydrogen bonding is indicated by red dashed lines.

In light of previous observations, this paper reports the single-crystal X-ray structure of co-crystals of (1:1) 5-fluorocytosine/isocytosine monohydrate, (I). The solid-state arrangement of molecules of (I) has then been compared with the structurally related fluorocytosine/5-fluoroisocytosine monohydrate molecular complex, PANLAS [12]. The latter molecular complex differs from (I) in changing F/H atoms at the 5 position of isocytosine (Scheme 2).

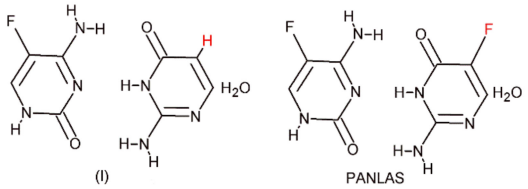

Scheme 2. Chemical components of the isomorphic and isostructural co-crystals of 5-fluorocytosine/isocytosine monohydrate, (I), and 5-fluorocytosine/5-fluoroisocytosine monohydrate, PANLAS.

The choice of the components of this binary co-crystal was made from consideration of the following points.

5-Fluorocytosine (Flucytosine) is a synthetic monofluorinated analog of cytosine. This compound can exist in different tautomeric forms, due to the presence of solvent-exchangeable protons. In the crystal, it exhibits polymorphism and is known only in the 1*H*-ketoamino form, the most stable tautomer in aqueous solution [13]. It is structurally very similar to its parent nucleobase and satisfies steric requirements at enzyme receptor sites, therefore it is commonly used as antimetabolite. Flucytosine can act as an antifungal agent, as it is deaminated by cytosine deaminase of the fungal cells to give 5-fluorouracil, resulting in RNA miscoding. 5-Fluorocytosine also plays an important role in the treatment of different types of cancer, although its use is limited by severe side effects [14].

Isocytosine (2-aminouracil), an isomer of cytosine, deserved special attention in experiments with an artificial pyrimidine base pair to expand the genetic alphabet of DNA, and to understand how the complementarity originally appeared in the form of the G–C [15]. Isocytosine is subject to prototropic tautomerism between the 1*H* and 3*H*-ketoamino forms, and it can form in solid-state intermolecular complexes with one or the other tautomer. In the 3*H*-ketoamino form, the most stable tautomer in polar solvents [16,17], isocytosine undergoes base pairing in a WC manner with unnatural isoguanine, and in a reversed WC manner with natural guanine, and has been used for structural studies of nucleic acids [18] as well as for hydrogen-bonding in nucleobases [19]. It has been shown that isocytosine could provide a base for a putative new prodrug 5-fluoroisocytosine, when used together with a putative isocytosine deaminase [20].

A search on the ConQuest module [21], version 2020.1.1 of the Cambridge Crystallographic Database (CSD version 5.41, August 2020 update) [22] for neutral 5-fluorocytosine and neutral isocytosine gave 14 hits. From this survey, 12 hits contained pure or solvate 5-fluorocytosine as 1*H*-ketoamino tautomer (refcodes: BIRMEU, BIRMEU01, BIRMEU02, BIRMEU03, DUKWAI, DUKWEW, DUKWIQ, MEBQEQ, MEBQEQ01, MEBQIU, MEBQOA, and MEBQUG [8,23–25]), and only two contained pure isocytosine as 1*H* or 3*H*-ketoamino tautomer (refcodes: ICYTIN and ICYTIN01 [26,27]).

In this work, analysis of the degree of similarity of (I) with PANLAS demonstrated that (1:1) 5-fluorocytosine/5-fluoroisocytosine monohydrate was the first example of isomorphic and isostructural co-crystals of pyrimidine nucleobases. The experimental results were complemented with Hirshfeld surface analysis to evaluate the contribution of different intermolecular interactions in the crystal packing.

Interestingly, in PANLAS, 5-fluoroisocytosine is present as a 3*H*-ketoamino tautomer, a tautomeric form never found in crystals of the isomer 5-fluorocytosine but observed for pure isocytosine. This tautomer favors pairing in the WC manner with 5-fluorocytosine through an intermolecular triple hydrogen bond. Any attempts to grow crystals to determine the solid-state structure of pure 5-fluoroisocytosine, which has not been reported so far, failed.

This article is a continuation of the work carried out in this laboratory on the design, solid-state synthesis and crystal structure determination of binary/ternary co-crystals of unnatural/5-halosubstituted nucleobases in which coformers are held together by hydrogen (or halogen) bonds [28–36].

2. Materials and Methods

2.1. Crystal Preparation

The 5-fluorocytosine and isocytosine were purchased from Aldrich (99% purity) and subjected to further purification by successive sublimation under reduced pressure. For the mechanochemical synthesis of co-crystals, equimolecular amounts (0.1 mmol in 1:1 stoichiometric ratio) of pure products were taken in an agate mortar and pestle, and then mixed and ground manually without the addition of any solvent. Crystallization of the ground powder was adjusted in methanol. The resulting solution (1 mL) was heated at 60 °C with continuous stirring for 6 h under reflux, and then slowly cooled to room temperature and filtered. Single crystals were obtained via slow evaporation of methanol solution at room temperature after ca three days.

2.2. Single Crystal Structure Analysis

The details of crystal data, data collection and structure refinement are summarized in Table 1. The data set was collected on an Xcalibur S CCD diffractometer (graphite-monochromated Mo Kα radiation, λ = 0.710689 Å) at room temperature using the *CrysAlisPro* software package (Rigaku Oxford Diffraction, Yarnton, United Kingdom, 2018) [37]. The crystal structure was solved by direct methods using SIR2004 [38]. All the non-hydrogen atoms were refined anisotropically by the full-matrix least-squares method based on F^2 using SHELXL-2014/7 [39], within the WinGX system [40]. All H atoms were found through difference Fourier, but for refinement all C-bound H atoms were placed in calculated positions, with C–H = 0.93 Å and U_{iso} (H) = 1.2U_{eq} of the parent C atom, and refined as riding on the adjacent atoms. Positional and isotropic thermal parameters of H atoms of the heteroatoms were freely refined, giving N–H and O–H (water molecule) distances in the range 0.89 (3)–0.94 (3) and 0.87 (4)–0.88 (4) Å, respectively. The molecular and packing diagrams were prepared using the Mercury 3.9 program package [41]. The Hirshfeld surface analysis was carried out using *Crystal Explorer17* (University of Western Australia, Crawley, AU, Australia [42]). The Cambridge Crystallographic Data Centre (CCDC) 2032880 contains the supplementary crystallographic data for this paper. These data can be obtained free of charge via http://www.ccdc.cam.ac.uk/conts/retrieving.html (or from the CCDC, 12 Union Road, Cambridge, CB2 1EZ, United Kingdom; Fax: +44 1223 336033; Email: deposit@ccdc.cam.ac.uk).

Table 1. Crystal data, data collection, and refinement for compound (I).

Crystal Data.	
Chemical formula	$C_4H_4FN_3O{\cdot}C_4H_5N_3O{\cdot}H_2O$
M_r	258.23
Crystal system, space group	Triclinic, *P*-1
Temperature (K)	298
a, *b*, *c* (Å)	5.3363 (9), 8.3389 (17), 12.6501 (12)
a, b, g (°)	93.009 (12), 92.037 (11), 100.837 (15)
V (Å^3)	551.52 (15)
Z	2
Radiation type	Mo *Ka*
m (mm^{-1})	0.13
Crystal size (mm)	0.10 × 0.08 × 0.07
Data collection	
T_{min}, T_{max}	0.702, 1.000
No. of measured, independent, and observed [$I > 2s(I)$] reflections	5277, 2042, 1401
R_{int}	0.037
(sin q/l)$_{max}$ (Å^{-1})	0.606
Refinement	
$R[F^2 > 2s(F^2)]$, $wR(F^2)$, *S*	0.063, 0.164, 1.07
No. of parameters	195
Dr_{max}, Dr_{min} (e Å^{-3})	0.26, −0.24

3. Results and Discussion

3.1. Structural Analysis

The title compound, (I), crystallized in the triclinic centrosymmetric space group P-1, and the asymmetric unit comprised of two molecules of 5-fluorocytosine and isocytosine and one water molecule of crystallization (Figure 2). In (I), as found for pure coformers, only the aminooxo tautomers were observed, with the N1a and N3 positions carrying the acidic proton. As already mentioned, in the solid state 5-fluoroisocytosine was present only in the 1*H*-ketoamino form, whereas isocytosine had two stable 1*H* and 3*H*-ketoamino tautomers. In the title compound, the presence of isocytosine as 3*H*-ketoamino tautomer favored the formation of almost-coplanar WC base pairs with 5-fluorocytosine (the two molecules being inclined by 5.4 (1)° to one another) through a DAA/ADD hydrogen-bonding pattern (three-point interaction, TPI) of $R^2_2(12)$ graph-set motif [43–45]. The values of bond lengths and angles agreed with those of the corresponding geometrical parameters found in the crystal structures showing 5-fluorocytosine monohydrate [8,23,24] and isocytosine [26,27] as 1*H* and 3*H*-ketoamino tautomers, respectively.

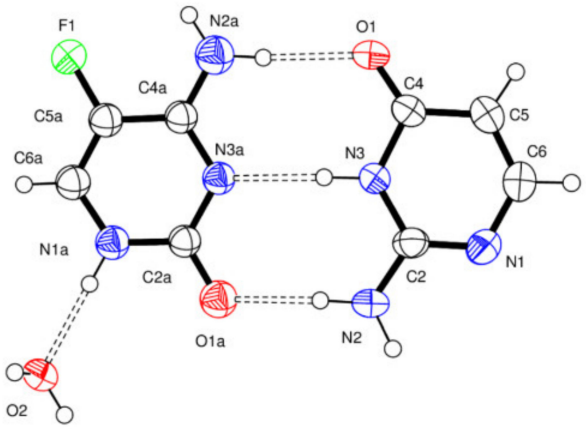

Figure 2. The asymmetric unit of (I), showing the adopted atom-numbering scheme. Displacement ellipsoids are at the 50% probability level. The asymmetric unit was selected so that the nucleobase molecules were linked by triple hydrogen bonds. H atoms are shown as small spheres of arbitrary radii. Hydrogen bonding is indicated by dashed lines.

Analysis of crystal structure similarity (CSS) was undertaken for the pair PANLAS/(I), using the graphical user interface of the Mercury program (CSD version 2020.2.0, Materials module). With this methodology, based on the COMPACK algorithm [46], from each CIF file a cluster of molecules (default size equal to 15) was obtained by picking a molecule plus a number of its closest neighboring molecules, and analyzing the overlapping molecules in the two clusters was then attempted. Two crystal structures are isostructural to within a specified tolerance (the default distance and angle tolerances being 20% and 20°, respectively) if, by comparing a cluster of 15 molecules, the algorithm returns 15 out of 15 molecules in common within the tolerance parameters set. The root mean square deviations in atomic positions (RMSD) were then calculated for the overlapping molecules in the two clusters. Analysis of the PXRD pattern was also performed using the already-cited CSD Materials module. With this method, the comparison of simulated PXRD patterns from each CIF file returned a similarity index (PXS) which ranged from 0 (completely dissimilar patterns) to 1 (identical patterns). These similarity methods were applied to the pair PANLAS/(I) for the comparison of a cluster extended to 20 molecules, as more than one molecule was present in the asymmetric unit [47]. The calculations of CSS, PXS and RMSD showed that the central molecule plus 19 symmetry-related molecules were in a common packing shell (Table 2).

Table 2. Packing similarity in matched crystal structures of PANLAS and (I) co-crystals.

	Unit-Cell Parameters	RMSD (Å)	PXS	*P*
PANLAS				
a, *b*, *c* (Å)	5.4122 (16), 8.447 (2), 12.083 (4)			
a, *b*, *g* (°)	89.454 (5), 85.718 (5), 77.096 (4)			
V (Å^3)	536.9 (3)	0.212	0.943	0.014
(I)				
a, *b*, *c* (Å)	5.3363 (9), 8.3389 (17), 12.6501 (12)			
a, *b*, *g* (°)	93.009 (12), 92.037 (11), 100.837 (15)			
V (Å^3)	551.52 (15)			

Comparison of the simulated PXRD patterns shows some differences (Figure 3), as PXRD is sensitive to chemical composition and even to small variations in cell metrics and atomic displacement parameters originated by data collection performed under different temperatures (PANLAS, 150 K; (I), 298 K) [47], but results returned by similarity methods suggests that these co-crystals have the same crystal packing.

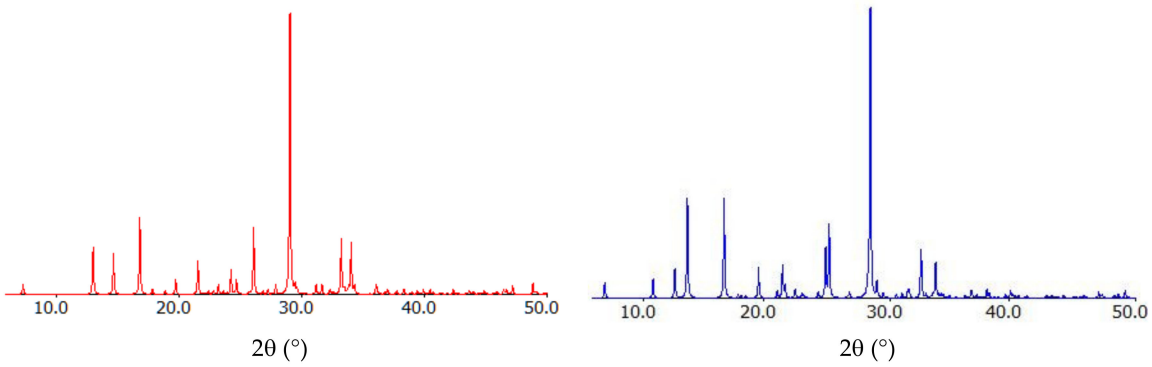

Figure 3. Simulated PXRD patterns for PANLAS (red) and (I) (blue).

The isomorphism of the crystal structures was determined by using the unit-cell parameters of the two crystal structures to calculate the unit-cell similarity index (Π) [48]. If Π = 0, then the matched crystal structures are isomorphous. In the present case, the Π index was close to zero (zero up to the first decimal place), suggesting the isomorphism of the pair PANLAS/(I) (Table 2).

Taken together, all these results indicated (1:1) 5-fluorocytosine/isocytosine monohydrate to be isomorphic and isostructural with (1:1) 5-fluorocytosine/5-fluoroisocytosine monohydrate molecular (Figure 4), which differed solely in the H/F substitution at the C5 position of isocytosine. Neither of the two atoms was involved in the hydrogen bonding as donor or acceptor functional groups, although the F···F close contact [2.9003 (15) Å] observed in PANLAS between adjacent TPI dimers within a ribbon was replaced in (I) by the F···H contact (3.175 Å).

Crystal packing is mainly controlled by interactions between nucleobases, and the hydrogen-bonding scheme (Table 3) shows that TPI pairs and water molecules have the dual role of hydrogen bond donors and acceptors. Specifically, ribbons running approximately along the c axis were formed by two different $R^2_4(8)$ hydrogen bond rings which involved strong N–H···O (carbonyl) hydrogen bonds of adjacent antiparallel TPI heterodimers (Figure 4a). Nonetheless, water molecules play a fundamental role in the hydrogen bonding interactions, which include four intermolecular contacts. Acting as both hydrogen bond donors and acceptors, water molecules join together two TPI heterodimers by forming $R^3_3(10)$ hydrogen bond rings within a ribbon. Moreover, water molecules interact as hydrogen bond acceptors with a third TPI heterodimer from an adjacent ribbon through weak C–H···O intermolecular interactions, favoring the formation of

a two-dimensional network. Neighboring networks are held together by water-mediated Ow–O hydrogen bonds (Figure 4b).

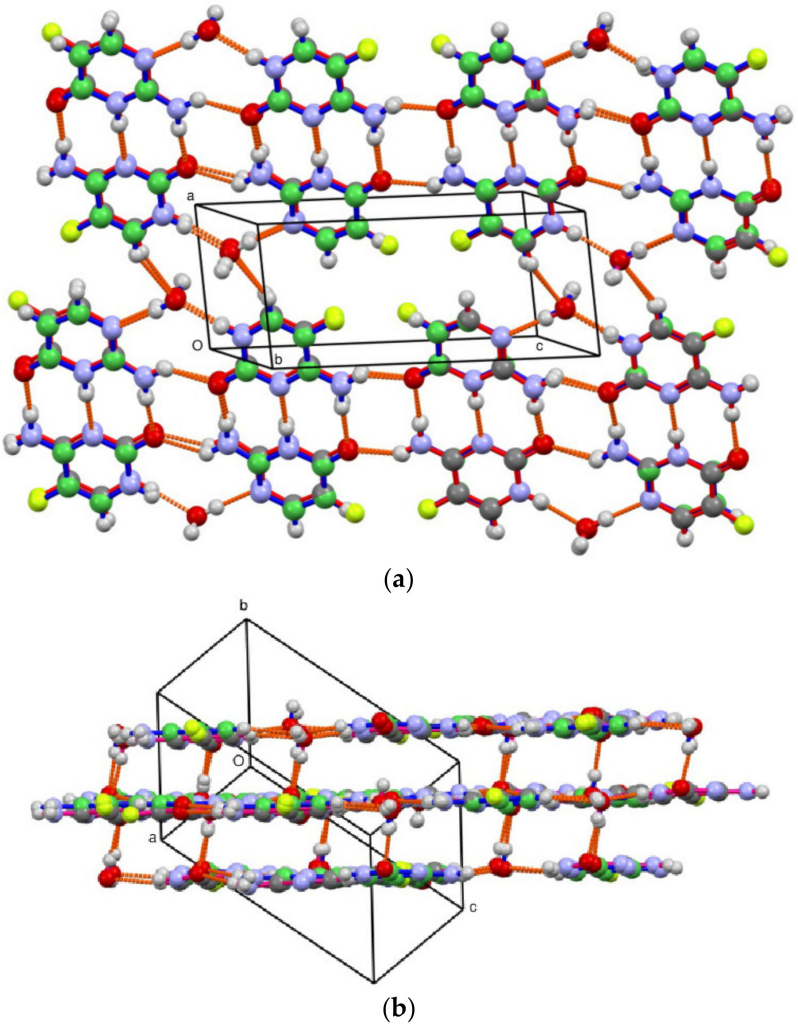

Figure 4. Cluster overlay of PANLAS and (I), showing crystal packing similarity: (**a**) hydrogen-bonded ribbons viewed approximately down b; (**b**) ribbons hydrogen bonded via water molecules viewed approximately parallel to the bc plane. Bonds of molecules of PANLAS have been colored red, bonds of molecules of the title compound are blue. All atoms are shown as small spheres of arbitrary radii. Hydrogen bonding is indicated by orange dashed lines.

Table 3. Hydrogen-bond geometry (Å,º) for (I).

D–H···*A*	*D*–H	H···*A*	*D*···*A*	*D*–H···*A*
N2–H2*A*···O1*A*	0.94 (3)	1.99 (3)	2.920 (3)	173 (3)
N2–H2*B*···O1*A* [i]	0.92 (3)	2.09 (3)	2.868 (3)	142 (2)
N3–H3···N3*A*	0.94 (3)	2.01 (3)	2.946 (3)	175 (2)
N2*A*–H2*AA*···O1 [ii]	0.90 (3)	2.03 (3)	2.830 (3)	147 (2)
N2*A*–H2*AB*···O1	0.91 (3)	2.03 (3)	2.930 (3)	171 (2)
N1*A*–H*N*1*A*···O2	0.89 (3)	1.93 (3)	2.816 (3)	171 (2)
C6*A*–H6*A*···O2 [iii]	0.93	2.42	3.267 (3)	151
O2–H21*W*···N1 [i]	0.88 (4)	1.93 (4)	2.807 (3)	175 (3)
O2–H22*W*···O1*A* [iv]	0.87 (4)	1.97 (4)	2.841 (3)	175 (4)

Symmetry codes: (i) −*x*−1, −*y*+1, −*z*+2; (ii) −*x*−1, −*y*, −*z*+1; (iii) −*x*−3, −*y*, −*z*+2; (iv) *x*−1, *y*, *z*.

3.2. Hirshfeld Surface Analysis

The 3D Hirshfeld surface, mapped over normalized contact distance d_{norm} [49], and the 2D fingerprint plots, which give the contribution of the interatomic contacts to the Hirshfeld surface, are shown in Figure 5. The most prominent interactions, due to N–H···O intermolecular hydrogen bonds, are shown by large and deep red spots on the surface. The H···H contacts, representing van der Waals interactions, were the most populated contacts and contributed 28.9% of the total intermolecular contacts. The abundance of the O···H/H···O (18.9%) and N···H/H···N (14.3%) contacts confirmed that intermolecular hydrogen bond interactions play important roles in the crystal packing. Lower percentages were found for C···H/H···C (11.5%) and F···H/H···F (10.7%). The contributions of the N···C/C···N (3.9%), O···C/C···O (3.4%), C···C (2.0%), O···N/N···O (1.8%), N···F/F···N (1.7%) and C···F/F···C (1.7%) also supplement the overall crystal packing. Other intermolecular contacts contributed less than 2% to the Hirshfeld surface mapping.

The replacement in PANLAS of the H atom by the F atom at the 5 position of isocytosine affected, as expected, the contribution of the contacts involving the above-mentioned atoms. In passing from PANLAS to (I), the decrease in the contribution for the H···H, C···H/H···C and N···H/H···N contacts (−6.5, −2.7 and −1.7%, respectively) was essentially balanced with the increase for the C···F/F···C, N···F/F···N, F···F, O···F/F···O and H···F/F···H (+3.3, 1.6, 1.5, 1.2 and 0.5%, respectively).

4. Conclusions

In summary, in this work the crystal structure of (1:1) 5-fluorocytosine/isocytosine monohydrate molecular complex has been analyzed in terms of spatial disposition and compared with that of the structurally-related fluorocytosine/5-fluoroisocytosine monohydrate molecular complex. From the evaluation of results obtained with the similarity methods, it has been shown that this molecular complex exhibits isomorphism and isostructurality with (1:1) 5-fluorocytosine/5-fluoroisocytosine monohydrate molecular complex. The crystal structure was sustained by the base-pairing interaction between the 1*H*-ketoamino form of 5-fluorocytosine and the 3*H*-ketoamino form of isocytosine, demonstrating that complementary binding enables the crystallization of specific tautomers. The robustness of the supramolecular architectures based on three-point recognition synthon, which benefits from the presence of isocytosine in the 3*H*-ketoamino form, was responsible of the existence of isostructurality between (I) and PANLAS. Indeed, particularly in the presence of strong interactions such as TPI, no change in the supramolecular arrangement due to the substitution of the H atom with the fluorine atom is expected, if neither of the two atoms are involved in hydrogen bonding as donor or acceptor functional groups [50]. The solidity of triple hydrogen-bonding interaction has been invoked to tolerate the H/F exchange in isostructural co-crystals of (1:1) barbiturate melamine complexes [51].

The understanding of changes in noncovalent interactions induced by chemical modifications of nucleobases is essential for investigating molecular recognition processes involved in DNA/RNA base pairing. Therefore, crystal structure determination of molecular complexes of nucleobases with their fluorinated derivatives, where covalently bound fluorine atoms cannot compete with stronger heteroatoms as acceptors in the formation of hydrogen bonds [52,53], can provide important experimental insights into the nature of DNA/RNA pairing interactions between natural bases and their close unnatural analogs [54].

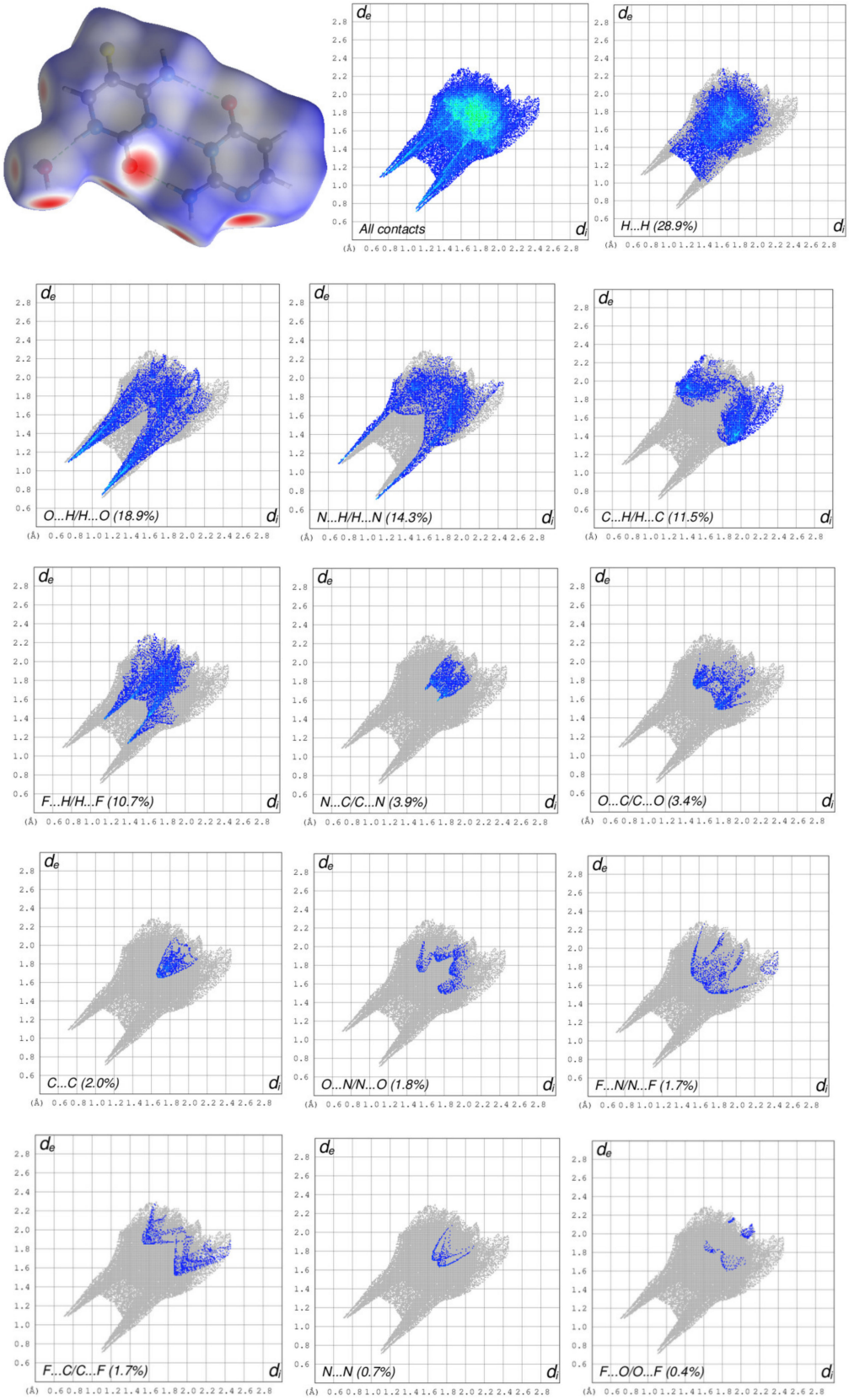

Figure 5. Hirshfeld surfaces mapped on d_{norm} [color scale: −0.6250 (red), 1.2492 a.u. (blue)] and decomposed two-dimensional fingerprint plots for (I). Various close contacts and their proportional contributions are reported. Other (not shown) intermolecular contacts contributed approximately less than 1% to the Hirshfeld surface mapping.

Funding: This research received no external funding.

Conflicts of Interest: The author declares no conflict of interest.

References

1. Kálmán, A.; Párkányi, L.; Argay, G. Classification of the isostructurality of organic molecules in the crystalline state. *Acta Crystallogr. Sect. B Struct. Sci.* **1993**, *49*, 1039–1049. [CrossRef]
2. Ranjan, S.; Devarapalli, R.; Kundu, S.; Saha, S.; Deolka, S.; Vangala, V.R.; Reddy, C.M. Isomorphism: 'Molecular similarity to crystal structure similarity' in multicomponent forms of analgesic drugs tolfenamic and mefenamic acid. *IUCrJ* **2020**, *7*, 173–183. [CrossRef]
3. Corpinot, M.K.; Guo, R.; Tocher, D.A.; Buanz, A.B.M.; Gaisford, S.; Price, S.L.; Bučar, D.-K. Are Oxygen and Sulfur Atoms Structurally Equivalent in Organic Crystals? *Cryst. Growth Des.* **2017**, *17*, 827–833. [CrossRef]
4. Giangreco, I.; Cole, J.C.; Thomas, E. Mining the Cambridge Structural Database for Matched Molecular Crystal Structures: A Systematic Exploration of Isostructurality. *Cryst. Growth Des.* **2017**, *17*, 3192–3203. [CrossRef]
5. Valinluck, V.; Liu, P.; Kang, J.I.; Burdzy, A.; Sowers, L.C. 5-Halogenated pyrimidine lesions within a CpG sequence context mimic 5-methylcytosine by enhancing the binding of the methyl-CpG-binding domain of methyl-CpG-binding protein 2 (MeCP2). *Nucleic Acids Res.* **2005**, *33*, 3057–3064. [CrossRef]
6. Byun, J.; Henderson, J.P.; Heinecke, J.W. Identification and quantification of mutagenic halogenated cytosines by gas chromatography, fast atom bombardment, and electrospray ionization tandem mass spectrometry. *Anal. Biochem.* **2003**, *317*, 201–209. [CrossRef]
7. Braun, D.E.; Kahlenberg, V.; Griesser, U.J. Experimental and Computational Hydrate Screening: Cytosine, 5-Flucytosine, and Their Solid Solution. *Cryst. Growth Des.* **2017**, *17*, 4347–4364. [CrossRef] [PubMed]
8. Hulme, A.T.; Tocher, D.A. The Discovery of New Crystal Forms of 5-Fluorocytosine Consistent with the Results of Computational Crystal Structure Prediction. *Cryst. Growth Des.* **2006**, *6*, 481–487. [CrossRef]
9. Braun, D.E.; Griesser, U.J. Prediction and experimental validation of solid solutions and isopolymorphs of cytosine/5-flucytosine. *CrystEngComm* **2017**, *19*, 3566–3572. [CrossRef] [PubMed]
10. Portalone, G.; Moilanen, J.O.; Tuononen, H.M.; Rissanen, K. Role of Weak Hydrogen Bonds and Halogen Bonds in 5-Halo-1,3-dimethyluracils and Their Cocrystals—A Combined Experimental and Computational Study. *Cryst. Growth Des.* **2016**, *16*, 2631–2639. [CrossRef]
11. Khomenko, V.G.; Mitkevich, V.V.; Sukhodub, L.F. The crystal structures of two methyl derivatives of uracil with C–H···O hydrogen bonding. *Bull. Nat. Acad. Sci. Ukraine: Geol. Chem. Biol. Sci.* **1986**, *10*, 34–37.
12. Hulme, A.T.; Tocher, D.A. 4-Amino-5-fluoropyrimidin-2(1H)-one-2-Amino-5-fluoropyrimidin-4(3H)-one-water (1/1/1). *Acta Cryst.* **2005**, *61*, o2112–o2113. [CrossRef]
13. Mohammad-Hasani, E.; Beyramabadi, S.A.; Pordel, M. Tautomerism and non-covalent interactions of flucytosine with armchair (5,5) SWCNT and γ-Fe_2O_3 nanoparticles: A DFT study. *Indian J. Chem.* **2017**, *56*, 626–632.
14. Vermes, A.; Guchelaar, H.J.; Dankert, J. Flucytosine: A review of its pharmacology, clinical indications, pharmacokinetics, toxicity and drug interactions. *J. Antimicrob. Chemother.* **2000**, *46*, 171–179. [CrossRef]
15. Hirao, I.; Kimoto, M.; Yamashige, R. Natural versus Artificial Creation of Base Pairs in DNA: Origin of Nucleobases from the Perspectives of Unnatural Base Pair Studies. *Acc. Chem. Res.* **2012**, *45*, 2055–2065. [CrossRef] [PubMed]
16. Gorb, L.; Podolyan, Y.; Leszczynski, J. A theoretical investigation of tautomeric equilibria and proton transfer in isolated and monohydrated cytosine and isocytosine molecules. *J. Mol. Struct. THEOCHEM* **1999**, *487*, 47–55. [CrossRef]
17. Pohl, R.; Socha, O.; Sala, M.; Rejman, D.; Dračínský, M. The Control of the Tautomeric Equilibrium of Isocytosine by Intermolecular Interactions. *Eur. J. Org. Chem.* **2018**, *2018*, 5128–5135. [CrossRef]
18. Yang, X.-L.; Sugiyama, H.; Ikeda, S.; Saito, I.; Wang, A.H.-J. Structural Studies of a Stable Parallel-Stranded DNA Duplex Incorporating Isoguanine:Cytosine and Isocytosine:Guanine Basepairs by Nuclear Magnetic Resonance Spectroscopy. *Biophys. J.* **1998**, *75*, 1163–1171. [CrossRef]
19. Camacho-García, J.; Montoro-García, C.; López-Pérez, A.M.; Bilbao, N.; Romero-Pérez, S.; González-Rodríguez, D. Synthesis and complementary self-association of novel lipophilic π-conjugated nucleoside oligomers. *Org. Biomol. Chem.* **2015**, *13*, 4506–4513. [CrossRef] [PubMed]
20. Aučynaitė, A.; Rutkienė, R.; Tauraitė, D.; Meškys, R.; Urbonavičius, J. Discovery of Bacterial Deaminases That Convert 5-Fluoroisocytosine Into 5-Fluorouracil. *Front. Microbiol.* **2018**, *9*, 2375. [CrossRef]

21. Bruno, I.J.; Cole, J.C.; Edgington, P.R.; Kessler, M.; Macrae, C.F.; McCabe, P.; Pearson, J.; Taylor, R. New software for searching the Cambridge Structural Database and visualizing crystal structures. *Acta Crystallogr. Sect. B Struct. Sci.* **2002**, *58*, 389–397. [CrossRef]
22. Groom, C.R.; Bruno, I.J.; Lightfoot, M.P.; Ward, S.C. The Cambridge Structural Database. *Acta Crystallogr. Sect. B Struct. Sci. Cryst. Eng. Mater.* **2016**, *72*, 171–179. [CrossRef]
23. Louis, T.; Low, J.N.; Tollin, P. 5-Fluorocytosine. *Cryst. Struct. Commun.* **1982**, *11*, 1059–1064.
24. Portalone, G.; Colapietro, M. Redetermination of 5-fluorocytosine monohydrate. *Acta Crystallogr. Sect. E Struct. Rep. Online* **2006**, *62*, 1049–1050. [CrossRef]
25. Tutughamiarso, M.; Bolte, M.; Egert, E. New pseudopolymorphs of 5-fluorocytosine. *Acta Crystallogr. Sect. C Cryst. Struct. Commun.* **2009**, *65*, o574–o578. [CrossRef]
26. Sharma, B.D.; McConnell, J.F. The crystal and molecular structure of isocytosine. *Acta Crystallogr.* **1965**, *19*, 797–806. [CrossRef]
27. Portalone, G.; Colapietro, M. Redetermination of isocytosine. *Acta Crystallogr. Sect. E Struct. Rep. Online* **2007**, *63*, o1869–o1871. [CrossRef]
28. Brunetti, B.; Portalone, G.; Piacente, V. Sublimation Thermodynamic Parameters for 5-Fluorouracil and Its 1-Methyl and 1,3-Dimethyl Derivatives from Vapor Pressure Measurements. *J. Chem. Eng. Data* **2002**, *47*, 17–19. [CrossRef]
29. Portalone, G.; Colapietro, M. First example of cocrystals of polymorphic maleic hydrazide. *J. Chem. Crystallogr.* **2004**, *34*, 609–612. [CrossRef]
30. Portalone, G.; Colapietro, M. Asymmetric base pairing in the complex 5-fluorocytosinium chloride/5-fluorocytosine monohydrate. *J. Chem. Crystallogr.* **2006**, *37*, 141–145. [CrossRef]
31. Portalone, G.; Colapietro, M. Solid-Phase Molecular Recognition of Cytosine Based on Proton-Transfer Reaction. *J. Chem. Crystallogr.* **2008**, *39*, 193–200. [CrossRef]
32. Portalone, G. Supramolecular association in proton-transfer adducts containing benzamidinium cations. I. Four molecular salts with uracil derivatives. *Acta Crystallogr. Sect. C Cryst. Struct. Commun.* **2010**, *66*, o295–o301. [CrossRef]
33. Portalone, G. Solid-phase molecular recognition of cytosine based on proton-transfer reaction. Part II. supramolecular architecture in the cocrystals of cytosine and its 5-Fluoroderivative with 5-Nitrouracil. *Chem. Central J.* **2011**, *5*, 51. [CrossRef]
34. Portalone, G.; Irrera, S. Supramolecular structure of unnatural nucleobases: Revised structure of (2:1) 6-methylisocytosinium dihydrogen monophosphate adduct. *J. Mol. Struct.* **2011**, *991*, 92–96. [CrossRef]
35. Portalone, G.; Rissanen, K. Multifacial Recognition in Binary and Ternary Cocrystals from 5-Halouracil and Aminoazine Derivatives. *Cryst. Growth Des.* **2018**, *18*, 5904–5918. [CrossRef]
36. Portalone, G. Site Selectivity of Halogen Oxygen Bonding in 5- and 6-Haloderivatives of Uracil. *Crystals* **2019**, *9*, 467. [CrossRef]
37. CrysAlis, P.R.O. *Rigaku Oxford Diffraction*; Agilent Technologies UK Ltd.: Yarnton, UK, 2018.
38. Burla, M.C.; Caliandro, R.; Camalli, M.; Carrozzini, B.; Cascarano, G.L.; De Caro, L.; Giacovazzo, C.; Polidori, G.; Spagna, R. SIR2004: An improved tool for crystal structure determination and refinement. *J. Appl. Crystallogr.* **2005**, *38*, 381–388. [CrossRef]
39. Sheldrick, G.M. Crystal structure refinement with SHELXL. *Acta Crystallogr. Sect. C Struct. Chem.* **2015**, *C71*, 3–8. [CrossRef]
40. Farrugia, L.J. WingX and ORTEP for Windows: An update. *J. Appl. Cryst.* **2012**, *45*, 849–854. [CrossRef]
41. Macrae, C.F.; Bruno, I.J.; Chisholm, J.A.; Edgington, P.R.; McCabe, P.; Pidcock, E.; Rodriguez-Monge, L.; Taylor, R.; Van De Streek, J.; Wood, P.A. Mercury CSD 2.0—New features for the visualization and investigation of crystal structures. *J. Appl. Crystallogr.* **2008**, *41*, 466–470. [CrossRef]
42. Turner, M.J.; Mckinnon, J.J.; Wolff, S.K.; Grimwood, D.J.; Spackman, P.R.; Jayatilaka, D.; Spackman, M.A. CrystalExplorer17. The University of Western Australia. 2017. Available online: http://hirshfeldsurface.net (accessed on 2 November 2020).
43. Etter, M.C.; Macdonald, J.C.; Bernstein, J. Graph-set analysis of hydrogen-bond patterns in organic crystals. *Acta Crystallogr. Sect. B Struct. Sci.* **1990**, *46*, 256–262. [CrossRef]
44. Bernstein, J.; Davis, R.E.; Shimoni, L.; Chang, N.-L. Patterns in Hydrogen Bonding: Functionality and Graph Set Analysis in Crystals. *Angew. Chem. Int. Ed.* **1995**, *34*, 1555–1573. [CrossRef]

45. Motherwell, W.D.S.; Shields, G.P.; Allen, F.H. Visualization and characterization of non-covalent networks in molecular crystals: Automated assignment of graph-set descriptors for asymmetric molecules. *Acta Crystallogr. Sect. B Struct. Sci.* **1999**, *55*, 1044–1056. [CrossRef]
46. Chisholm, J.A.; Motherwell, S. COMPACK: A program for identifying crystal structure similarity using distances. *J. Appl. Crystallogr.* **2005**, *38*, 228–231. [CrossRef]
47. Sacchi, P.; Nauha, E.; Cruz-Cabeza, A.J.; Lusi, M.; Bernstein, J. Invitation to Submit: The Cambridge Structural Database Same or different—That is the question: Identification of crystal forms from crystal structure data. *CrystEngComm* **2020**. [CrossRef]
48. Oliveira, M.A.; Peterson, M.L.; Klein, D. Continuously Substituted Solid Solutions of Organic Co-Crystals. *Cryst. Growth Des.* **2008**, *8*, 4487–4493. [CrossRef]
49. Spackman, M.A.; Jayatilaka, D. Hirshfeld surface analysis. *CrystEngComm* **2009**, *11*, 19–32. [CrossRef]
50. Chopra, D.; Row, T.N.G. Role of organic fluorine in crystal engineering. *CrystEngComm* **2011**, *13*, 2175–2186. [CrossRef]
51. Nangia, A. Packing similarities in organic crystals with C–H/C–F exchange: A database analysis of CH3/CF3 pairs. *New J. Chem.* **2000**, *24*, 1049–1055. [CrossRef]
52. Dunitz, J.D.; Taylor, R. Organic Fluorine Hardly Ever Accepts Hydrogen Bonds. *Chem. Eur. J.* **1997**, *3*, 89–98. [CrossRef]
53. Dunitz, J. Organic fluorine: Odd man out. *ChemBioChem* **2004**, *5*, 614–621. [CrossRef] [PubMed]
54. Koller, A.N.; Božilović, J.; Engels, J.W.; Gohlke, H. Aromatic N versus aromatic F: Bioisosterism discovered in RNA base pairing interactions leads to a novel class of universal base analogs. *Nucleic Acids Res.* **2010**, *38*, 3133–3146. [CrossRef] [PubMed]